

Deep Learning Estimation of Small Airways Disease from Inspiratory Chest CT is Associated with FEV₁ Decline in COPD

Muhammad F. A. Chaudhary, Ph.D.,^{1,2,*,†}, Hira A. Awan, M.B.,^{1,*}, Sarah E. Gerard, Ph.D.,¹, Sandeep Bodduluri, Ph.D.,², Alejandro P. Comellas, M.D.,³, Igor Z. Barjaktarevic, M.D., Ph.D.,⁴, R. Graham Barr, M.D.,⁵, Christopher B. Cooper, M.D.,⁶, Craig J. Galban, Ph.D.,⁷, MeiLan K. Han, M.D.,⁸, Jeffrey L. Curtis, M.D.,⁸, Nadia N. Hansel, M.D.,⁹, Jerry A. Krishnan, M.D., Ph.D.,¹⁰, Martha G. Menchaca, M.D., Ph.D.,¹¹, Fernando J. Martinez, M.D.,¹², Jill Ohar, M.D.,¹³, Luis G. Vargas Buonfiglio, M.D.,¹⁴, Robert Paine, III, M.D.,¹⁴, Surya P. Bhatt, M.D.,², Eric A. Hoffman, Ph.D.,^{1,3,15}, and Joseph M. Reinhardt, Ph.D.^{1,15}

1. The Roy J. Carver Department of Biomedical Engineering, University of Iowa, Iowa City, IA, 52242.
2. Center for Lung Analytics and Imaging Research (CLAIR), Division of Pulmonary, Allergy and Critical Care Medicine, University of Alabama at Birmingham, Birmingham, AL 35294.
3. Department of Internal Medicine, Division of Pulmonary, Critical Care and Occupational Medicine, University of Iowa Roy J. and Lucille A. Carver College of Medicine, Iowa City, IA, 52242.
4. Division of Pulmonary and Critical Care Medicine, David Geffen School of Medicine at UCLA, Los Angeles, CA, 90095
5. Department of Epidemiology, Mailman School of Public Health, Columbia University, New York, NY, 10032.
6. Department of Physiology, David Geffen School of Medicine at UCLA, Los Angeles, CA, 90095.
7. Department of Radiology, University of Michigan, Ann Arbor, MI, 48109.
8. Division of Pulmonary and Critical Care Medicine, University of Michigan Health System, Ann Arbor, MI, 48109.
9. Department of Medicine, Johns Hopkins School of Medicine, Baltimore, MD, 21205.
10. Breathe Chicago Center, University of Illinois at Chicago, Chicago, IL, 60608.
11. Department of Radiology, College of Medicine, University of Illinois at Chicago, Chicago, IL, 60612.
12. University of Massachusetts Chan Medical School, Worcester, MA, 01655.

13. Wake Forest School of Medicine, Wake Forest University, Winston-Salem, NC, 27101.
14. Division of Respiratory, Critical Care and Occupational Pulmonary Medicine, University of Utah, Salt Lake City, UT, 84112.
15. Department of Radiology, University of Iowa Roy J. and Lucille A. Carver College of Medicine, Iowa City, IA, 52242.

Corresponding author: Joseph M. Reinhardt, Ph.D., The Roy J. Carver Department of Biomedical Engineering, 5601 Seamans Center, The University of Iowa, Iowa City, IA, 52242. Email: joe-reinhardt@uiowa.edu. Phone: +1 (319) 335-5634.

*Equal Contribution

[†]Muhammad F. A. Chaudhary is now at the Center for Lung Analytics and Imaging Research (CLAIR) at The University of Alabama at Birmingham. This study was conducted when he was at The Roy J. Carver Department of Biomedical Engineering at The University of Iowa.

Running Head: Deep learning fSAD and FEV₁ decline

Author Contributions:

Study concept and design: M.F.A.C., H.A.A., J.M.R.

Acquisition, analysis, or interpretation of data: all authors

Drafting of the manuscript: M.F.A.C, H.A.A., J.L.C, J.M.R.

Critical revision of the manuscript for important intellectual content: all authors

Statistical analysis: H.A.A., M.F.A.C.

Study supervision: J.M.R.

Manuscript Word Count: 3477 / 3500 (excluding *abstract, references, and legends*)

ABSTRACT

Rationale: Quantifying functional small airways disease (fSAD) requires additional expiratory computed tomography (CT) scan, limiting clinical applicability. Artificial intelligence (AI) could enable fSAD quantification from chest CT scan at total lung capacity (TLC) alone (fSAD^{TLC}).

Objectives: To evaluate an AI model for estimating fSAD^{TLC} and study its clinical associations in chronic obstructive pulmonary disease (COPD).

Methods: We analyzed 2513 participants from the SubPopulations and InteRmediate Outcome Measures in COPD Study (SPIROMICS). Using a subset ($n = 1055$), we developed a generative model to produce virtual expiratory CTs for estimating fSAD^{TLC} in the remaining 1458 SPIROMICS participants. We compared fSAD^{TLC} with dual volume, parametric response mapping fSAD^{PRM}. We investigated univariate and multivariable associations of fSAD^{TLC} with FEV₁, FEV₁/FVC, six-minute walk distance (6MWD), St. George's Respiratory Questionnaire (SGRQ), and FEV₁ decline. The results were validated in a subset ($n = 458$) from COPDGene study. Multivariable models were adjusted for age, race, sex, BMI, baseline FEV₁, smoking pack years, smoking status, and percent emphysema.

Measurements and Main Results: Inspiratory fSAD^{TLC} was highly correlated with fSAD^{PRM} in SPIROMICS (Pearson's $R = 0.895$) and COPDGene ($R = 0.897$) cohorts. In SPIROMICS, fSAD^{TLC} was associated with FEV₁ (L) (adj.β = -0.034, $P < 0.001$), FEV₁/FVC (adj.β = -0.008, $P < 0.001$), SGRQ (adj.β = 0.243, $P < 0.001$), and FEV₁ decline (mL / year) (adj.β = -1.156, $P < 0.001$). fSAD^{TLC} was also associated with FEV₁ (L) (adj.β = -0.032, $P < 0.001$), FEV₁/FVC (adj.β = -0.007, $P < 0.001$), SGRQ (adj.β = 0.190, $P = 0.02$), and FEV₁ decline (mL / year) (adj.β = -0.866, $P = 0.001$) in COPDGene. We found fSAD^{TLC} to be more repeatable than fSAD^{PRM} with intraclass correlation of 0.99 (95% CI: 0.98, 0.99) vs. 0.83 (95% CI: 0.76, 0.88).

Conclusions: Inspiratory fSAD^{TLC} captures small airways disease as reliably as fSAD^{PRM} and is associated with FEV₁ decline.

Word Count: 254 / 250

Funding Source: This work was supported by NHLBI grants R01 HL142625, U01 HL089897 and U01 HL089856, by NIH contract 75N92023D00011, and by a grant from The Roy J. Carver Charitable Trust (19-5154). The COPDGene study (NCT00608764) has also been supported by the COPD Foundation through contributions made to an Industry Advisory Committee that has

included AstraZeneca, Bayer Pharmaceuticals, Boehringer-Ingelheim, Genentech, GlaxoSmithKline, Novartis, Pfizer, and Sunovion.

INTRODUCTION

Small conducting airways of the lungs are the primary sites of airflow limitation in early obstructive lung disease (1, 2), and their loss is extensive by the time that airflow limitation is detectable by spirometry (3). Identifying early small airways disease (SAD) in susceptible individuals who have inhalational exposures linked to COPD is essential to the development of disease-modifying therapies for this leading cause of worldwide death and disability.

Currently, the only *in vivo* method to quantify SAD relies on image registration for demonstrating non-emphysematous air-trapping on chest computed tomography (CT) scans obtained at inspiration and expiration (4). These co-registered scans are analyzed through parametric response mapping (PRM) to quantify such air-trapping, termed functional small airways disease (fSAD^{PRM}) (4). MicroCT analysis of resected lungs demonstrated that fSAD^{PRM} accurately reflects SAD in advanced COPD (5). However, the need for additional expiratory CT incurs increased cost and ionizing radiation exposure. Additionally, expiratory CT scan acquisition in clinical settings requires specialized technician training and there is no harmonized protocol to coach and acquire images at different lung volumes (6). These drawbacks preclude application of PRM analysis to clinical settings where expiratory CT scans are unavailable. By contrast, inspiratory chest CT scans are common in many clinical settings, including lung cancer screening. Hence, a method for estimating fSAD from inspiratory chest CT scans alone would be valuable.

Deep generative modeling can reliably generate multimodal medical images by converting a medical image from one modality to the other (7). Recently, we developed a method for estimating an expiratory chest CT scan solely from a given inspiratory CT image (7). The synthesized virtual expiratory image could be used in combination with the available inspiratory CT scan for estimating SAD. We hypothesize that this single inspiratory volume fSAD estimation from chest CT at total lung capacity (TLC) can be used to identify regions of SAD and that these

regions will be associated with poor outcomes in COPD. To test our hypothesis, we analyzed data from the SubPopulations and InteRmediate Outcome Measures in COPD Study (SPIROMICS) cohort (8). The results were validated in a cohort from the Genetic Epidemiology of COPD (COPDGene) study (9). We also investigated the repeatability of inspiratory CT fSAD and compared its repeatability with the conventional fSAD^{PRM} extracted from two volumes.

METHODS

Study Populations

We analyzed data from the SubPopulations and InteRmediate Outcome Measures in COPD Study (SPIROMICS) which is a multicenter prospective cohort study being conducted at 14 clinical centers across the United States (US) (8). SPIROMICS enrolled 2981 participants between 40 and 80 years of age across four strata: with smoking history ≤ 1 pack-year (stratum 1) or a smoking history ≥ 20 pack-years (strata 2 – 4). The participants underwent high-resolution chest CT scans on full inspiration and expiration, i.e., at both total lung capacity (TLC) and residual volume (RV), respectively at their enrollment visit. We divided SPIROMICS participants as described below into two non-overlapping subsets, which were respectively used to train our generative model (to transform inspiratory CT to synthetic expiratory CT scans), and for the association of the resulting fSAD measurements from the single inspiratory and synthetic expiratory scans.

We externally validated our model on a subset from the Genetic Epidemiology of COPD (COPDGene) study (9). COPDGene is a multicenter observational cohort study that recruited nearly 10,300 participants across 21 clinical centers in the US. COPDGene used a different image acquisition protocol from SPIROMICS. COPDGene acquired chest CT scans at TLC and

functional residual capacity (FRC). However, in a sub-study at a single clinical site (Iowa), some participants were also scanned at RV ($n = 458$), and this group was used in this analysis.

Both studies were conducted according to the principles of the Helsinki accord. Written informed consent for both studies was provided by all participants, and the protocols were approved by the Institutional Review Boards (IRBs) of each participating study center.

Estimating fSAD from Inspiratory Chest CT

To synthesize virtual expiratory CT scans from a participant's inspiratory chest CT scan alone, we used a recently developed generative adversarial network (GAN), called LungViT (7). Before training the model, we registered the expiratory chest CT scan (treated as moving image) to the inspiratory chest CT scan (treated as the registration reference). We trained the generative model using registered scan pairs, obtained at TLC and RV, from SPIROMICS. The training set ($n = 1055$) comprised 55 individuals who never smoked, and 200 participants randomly sampled from each COPD Global Initiative for Chronic Lung Disease (GOLD) stage (0 – 4).

GANs use image pairs to learn a transformation from one image to the other, in our case, to transform TLC scans to RV scans. Generative models rely on two coupled neural networks, where an additional model (called the discriminator) is used to enhance and assess the image quality generated by the generative model (the generator) (7). Iterative feedback from the discriminator helps the generator to produce perceptually realistic images. Once trained, the generator can be used to synthesize a virtual chest CT scan at RV from a given TLC CT scan alone. For more details on model architecture and training please refer to the work in (7) and the online supplement.

Next, we used the trained generator to synthesize virtual expiratory chest CT scans for the remaining SPIROMICS ($n = 1458$) and COPDGene participants ($n = 458$). These virtual expiratory CT scans were employed, in combination with the TLC scans, to compute a variable called $fSAD^{TLC}$. We calculated $fSAD^{TLC}$ as the voxels between -950 HU to -810 HU on inspiratory chest CT scan and between -1000 HU to -857 HU on the virtual or synthetic expiratory CT scan (4, 10).

We compared the proposed $fSAD^{TLC}$ with the conventional dual volume, image registration-based $fSAD$, obtained using the PRM ($fSAD^{PRM}$). The $fSAD^{PRM}$ was computed by registering the expiratory CT scans at RV to the inspiratory CT scans at TLC. The $fSAD^{PRM}$ was defined as voxels between -950 HU and -810 HU on inspiratory chest CT and between -1000 HU and -857 HU on the expiratory CT (4, 10). The only difference between the $fSAD^{PRM}$ and $fSAD^{TLC}$ calculation was that the latter used a virtual expiratory CT scan at RV instead of the actual RV scan acquired by SPIROMICS. Both $fSAD^{PRM}$ and $fSAD^{TLC}$ were expressed as a percentage of total lung volume.

Predictors

Predictors in this study included age, sex, race, body mass index (BMI), smoking status (current or former defined as ≥ 6 -month cessation), smoking pack years, post-bronchodilator forced expiratory volume in 1 second (FEV_1), percent emphysema defined as percentage of low-attenuation areas (LAA%) below -950 Hounsfield units (HU), and $fSAD^{TLC}$ or $fSAD^{PRM}$.

Outcomes

We studied the association of $fSAD^{TLC}$ with various functional and clinical outcomes of respiratory morbidity in both SPIROMICS and COPDGene cohorts. Our study outcomes included lung

function measures such as the post-bronchodilator forced expiratory volume in 1 second (FEV₁) in liters (L) and the ratio of postbronchodilator FEV₁/FVC. We also analyzed the respiratory quality of life quantified by the total St. George's Respiratory Questionnaire (SGRQ) score (11). SGRQ score ranges between 0 and 100, where 0 indicates no symptom burden with a good quality of life, while 100 indicates a poor quality of patient life with high symptom burden (11). We also studied the association of fSAD^{TLC} with six-minute walk distance (6MWD) and mMRC (modified Medical Research Council) dyspnea scale that ranges from 0 to 4 in increasing order of shortness of breath (12).

In both cohorts, we further investigated the relationship between fSAD^{TLC} and change in FEV₁ between baseline and follow-up visit after five years. The change in FEV₁ was calculated as a difference between baseline FEV₁ and the follow-up FEV₁ around five years, which was then divided by the time between visits to calculate the change in mL / year.

Statistical Analysis

To initially investigate the relationship between percent fSAD^{TLC} and fSAD^{PRM}, we used Pearson's correlation. Scatter plots were also generated to assess if fSAD^{TLC} was able to reliably capture the distribution of fSAD^{PRM}. We also conducted a Bland-Altman analysis between the means of fSAD^{TLC} and fSAD^{PRM} to assess any systematic bias or variability in the differences across the range of measurements. Univariate and multivariable regression analysis was also conducted for investigating the association of fSAD^{TLC} with spirometry and clinical outcomes in COPD. We tested associations between baseline fSAD^{TLC} and post-bronchodilator FEV₁ (L) and FEV₁/FVC, with age, sex, race, body-mass index (BMI), smoking status, smoking pack years, and percent emphysema or LAA% as covariates. For assessing the association of baseline fSAD^{TLC} with

SGRQ, 6MWD (ft), and mMRC dyspnea scale, we added baseline post-bronchodilator FEV₁ (L) as an additional covariate for adjustment.

We studied the association of with change in FEV₁ (mL / year) after adjusting for the same set of variables mentioned above. We repeated the multivariable analysis for change in FEV₁ (mL / year) among GOLD 0 and GOLD 1 – 4 participants. To assess the relationship between fSAD^{TLC} and all-cause mortality, we categorized participants in four quartiles of fSAD^{TLC} and conducted Kaplan-Meier curve analysis for each quartile (13). Survival curves were plotted for each quartile, and the log-rank test was used to compare survival distributions across quartiles. All association studies and Kaplan-Meier curve analysis was repeated for the fSAD^{PRM}. A two-sided *P* value < 0.05 was considered to be significant.

Repeatability Analysis

We conducted a repeatability study to assess the overall reproducibility of fSAD^{TLC}. We used data from the SPIROMICS repeatability study that enrolled 100 participants at the primary study sites between 2012 and 2015 (14). The study participants were scanned at TLC and RV during their enrollment visit. Repeat scans at both TLC and RV were acquired 2 – 6 weeks after the enrollment visit (14). For both visits, we generated synthetic RV scans for computing fSAD^{TLC}. To test the repeatability of fSAD^{TLC}, we computed the intraclass correlation coefficient (ICC) using the single measurement, same raters' case (15). This was followed by a Bland-Altman analysis to test any systematic bias across the range of fSAD^{TLC}. ICC and Bland-Altman plots were also generated for fSAD^{PRM} to compare its repeatability with fSAD^{TLC}.

RESULTS

Study Design

SPIROMICS enrolled 2981 participants during its first phase from Nov 12, 2010, to July 31, 2015. Of 2981 participants, eight withdrew consent, and 1055 were reserved for training the TLC to RV generative model, as shown in **Figure E1**. Of 1918 scans, we removed 177 participants with change in TLC and RV volume less than 1L. After further eliminating the missing clinical information, we were able to obtain complete case data for 1458 participants at baseline in SPIROMICS (see **Figure E1**). At five-year follow-up, spirometry data was available only for 650 individuals (see **Figure E1**).

Of 10,305 individuals from the first phase of COPDGene, 473 had RV scans available for analysis at enrollment (see **Figure E1**). After eliminating the cases with missing clinical information, we analyzed baseline data from 458 participants to validate our results. For studying change in FEV₁, eight subjects were lost to follow-up at five years, as shown in **Figure E1**.

Participant Characteristics

The mean age at baseline was 62.9 (9.1) years in SPIROMICS and 63.3 (8.5) in COPDGene (see **Table 1**). Both cohorts were fairly balanced by biological sex with 788 (54%) and 215 (47%) males in SPIROMICS and COPDGene cohorts, respectively. In SPIROMICS, 588 (40%) individuals were current smokers, and the fraction was smaller for COPDGene with 130 (28%) individuals who smoked currently (see **Table 1**). As shown in **Table 1**, the mean baseline fSAD^{TLC} (%) in SPIROMICS was 12.98 (13.25) compared to a mean baseline fSAD^{PRM} (%) of 13.35 (12.21). Similarly, in COPDGene, the mean fSAD^{TLC} (%) was 9.55 (10.99) and the mean fSAD^{PRM}

(%) was 10.13. (9.46) (see **Table 1**). Participant characteristics at five-year follow-up are reported in **Table E1** of the online supplement.

Relationship between fSAD^{TLC} and fSAD^{PRM}

We show a qualitative comparison between the spatial distributions of fSAD^{PRM} and fSAD^{TLC} (see columns 4 and 5 in **Figure 1**) across three different SPIROMICS subjects with varying degrees of fSAD. We also show mid-coronal slices from the virtual RV images generated by our AI model (see column 3 in **Figure 1**). Perceptually, there were negligible differences between the real and virtual RV image slices, shown respectively in columns 2 and 3 of **Figure 1**). We observed a high Pearson's correlation between fSAD^{TLC} and fSAD^{PRM} in SPIROMICS ($R = 0.895$, $P < 0.001$) and COPDGene ($R = 0.897$, $P < 0.001$), suggesting a strong linear relationship between two variables (see **Figure 2A** and **2B**). Scatter plots showed a high agreement between the overall distributions of fSAD^{TLC} and fSAD^{PRM} in both cohorts (see **Figure 2A** and **2B**). Bland-Altman analysis between the means of fSAD^{TLC} and fSAD^{PRM} showed minimal bias of 0.37 and 0.58 in SPIROMICS (see **Figure 2C**) and COPDGene (see **Figure 2D**), respectively.

Lung Function and Respiratory Morbidity Predicted by fSAD^{TLC}

Univariate regression analysis suggested significant association of fSAD^{TLC} with lung function and respiratory morbidity in SPIROMICS and COPDGene cohorts (see **Tables E2** and **E3**). On multivariable analysis, fSAD^{TLC} was significantly associated with lung function measures in SPIROMICS: postbronchodilator FEV₁ (L) (adjusted $\beta = -0.034$, 95% CI: -0.037, -0.031; $P < 0.001$) and postbronchodilator FEV₁/FVC (adjusted $\beta = -0.008$, 95% CI: -0.008, -0.007; $P < 0.001$) (see **Table 2**), independent of age, sex, race, BMI, smoking status, pack years, BMI, and percent

emphysema. Similarly, fSAD^{TLC} was associated with FEV₁ (L) (adjusted $\beta = -0.032$, 95% CI: -0.038, -0.027; $P < 0.001$) and FEV₁ / FVC (adjusted $\beta = -0.007$, 95% CI: -0.008, -0.007; $P < 0.001$) in COPDGene (see **Table 3**). fSAD^{TLC} was also associated with SGRQ in SPIROMICS (adjusted $\beta = 0.240$, 95% CI: 0.127, 0.353, $P < 0.001$) and COPDGene (adjusted $\beta = 0.190$, 95% CI: 0.030, 0.350, $P = 0.02$). To compare fSAD^{TLC} with fSAD^{PRM}, we repeated the association studies for fSAD^{PRM} as well (see **Tables 2 and 3**). A Kaplan-Meier curve analysis revealed significantly increased rates of mortality (log rank $P < 0.001$) in individuals with increased fSAD^{TLC} (see **Figure 3**).

Change in FEV₁ and fSAD^{TLC}

In both SPIROMICS ($\beta = -1.156$, 95% CI: -1.699, -0.613; $P < 0.001$) and COPDGene ($\beta = -0.866$, 95% CI: -1.386, -0.345; $P < 0.001$), fSAD^{TLC} was significantly associated with change in FEV₁ (mL / year) for all subjects (see **Table 4**). We conducted stratified linear regression analysis for GOLD 0 and GOLD 1 – 4 to investigate the impact of fSAD^{TLC} on FEV₁ decline based on baseline airflow limitation (see **Table 4**). In both cohorts, fSAD^{TLC} was associated with FEV₁ decline for GOLD 1 – 4 participants (see **Table 4**). In SPIROMICS, for every additional 1% increase in fSAD^{TLC}, a decline in FEV₁ of 1.050 mL / year ($P = 0.001$) was observed for GOLD 1 – 4 participants. Similarly, in COPDGene, for a 1% increase fSAD^{TLC}, FEV₁ declined by 1.175 mL / year ($P = 0.003$) (see **Table 4**).

Repeatability of fSAD^{TLC}

Over a short follow-up of 2 – 6 weeks, we observed fSAD^{TLC} to be highly repeatable with ICC of 0.99 (95% CI: 0.98, 0.99). This was significantly higher than the ICC of fSAD^{PRM} (0.83 (95% CI:

0.76, 0.88)). A Bland-Altman analysis between the fSAD^{TLC} and fSAD^{PRM} computed at visit 1 and visit 2 chest CT scans from the SPIROMICS Repeatability study revealed minimal bias for both fSAD^{PRM} (0.26) and fSAD^{TLC} (0.22) (see **Figure 4A** and **4B**). The limits of agreement were significantly larger for fSAD^{PRM} (18%) as compared to fSAD^{TLC} (5%), suggesting greater overall variability in fSAD^{PRM} between 2 – 6 weeks follow-up.

Discussion

We aimed to determine whether generative AI can be used to derive fSAD from a single CT scan at TLC, and whether this single volume fSAD estimation correlates with clinical and functional outcomes in COPD. Traditionally, fSAD estimation has relied on an additional expiratory CT scan, a requirement that limits its clinical applicability (4, 10). We believe this is the first study to utilize a generative AI model for estimating fSAD from a single inspiratory CT scan. We demonstrated that, in two large cohorts, fSAD measured by TLC CT alone is associated with poor lung function, respiratory quality of life, and FEV₁ decline.

A comparison of fSAD^{TLC} and fSAD^{PRM} suggested a strong linear relationship between the two measurements, supporting our hypothesis that SAD can be accurately measured from TLC CT using generative AI. During training, our model learned to transform TLC scans to RV scans from a large number of TLC and RV pairs. Exposing our model to a large training dataset improved virtual RV image generation, allowing us to capture SAD from TLC as accurately as fSAD^{PRM}. An equally strong relationship between fSAD^{TLC} and fSAD^{PRM} was observed in the COPDGene cohort suggested model generalizability to different cohort. For both cohorts, Bland-Altman analysis between the means of percent fSAD^{TLC} and fSAD^{PRM} showed minimal bias across the range of two measurements, and the limits of agreement, while not too narrow, were reasonable,

suggesting that the two methods are generally consistent and could potentially be used interchangeably within an acceptable range.

We demonstrated that $fSAD^{TLC}$ was significantly associated with FEV_1 decline in both SPIROMICS and COPDGene cohorts. Our findings were consistent with those of Bhatt *et al.*, who found similar associations of $fSAD^{PRM}$ with FEV_1 decline in COPDGene (16). Further, in individuals with established airflow limitation and mild-to-severe COPD (GOLD 1 – 4), $fSAD^{TLC}$ was strongly associated with FEV_1 decline independent of baseline percent emphysema. This suggested that there was an involvement of a small airways disease component at baseline contributing towards FEV_1 decline. A consistency of these findings with $fSAD^{PRM}$ indicated the potential of single chest CT volume $fSAD^{TLC}$ as an alternative for characterizing disease progression in COPD. For both univariate and multivariable models, the direction of regression coefficients were consistent, and magnitudes were comparable between $fSAD^{TLC}$ and $fSAD^{PRM}$. This suggested a consistent influence of unit change in $fSAD^{TLC}$ and $fSAD^{PRM}$ on the outcome variables further signifying an agreement between them.

An important part of this study was the repeatability analysis conducted using data short-term follow-up data from the SPIROMICS Repeatability study (14). The repeat scans over short follow-up prevented any long-term variabilities that might occur due to disease. $fSAD^{TLC}$ was significantly more repeatable than $fSAD^{PRM}$, however, this was expected due to the potential for variations in patient effort between the repeat RV scans. Less common acquisition of RV scans in clinical practice results in inadequate coaching to expiratory volumes (RV and FRC), making them hard to reproduce. Since $fSAD^{PRM}$ relies on RV scans, its repeatability is more dependent on adequate patient effort each time they are being scanned. Since expiration scans are thus harder to reproduce (14), this complicates the repeatability of $fSAD^{PRM}$. On the contrary, the proposed

fSAD^{TLC} relies only on inspiratory chest CT scans, which are more easily reproducible and less prone to inadequate patient effort (17). These findings were also consistent with the results from the Repeatability Study where the dual volume CT biomarkers showed significantly lower ICC values compared to single volume metrics (14).

A few limitations of this study need to be recognized. Our spatial estimation of fSAD^{TLC} consistent with fSAD^{PRM} with a few differences in some isolated regions. Still, the major fSAD clusters were picked up by our method. We developed our model using scans from the SPIROMICS study that were acquired using a quality-controlled imaging protocol. This may not be true for the TLC scans acquired in clinical settings. It would be important to test our method in TLC scans with lower dosage and different acquisition protocols. We had to remove subjects with unreliable TLC or RV (volume difference < 1L) and acknowledge this as a quality control step in our analysis; fortunately, only 10% of the scans were considered unusable. For assessing change in FEV₁, we were limited to only two lung function measurements separated by a follow-up of almost five years. Another limitation of our method was that all the scans were acquired without any contrast agent, and whether these results are reproducible in CT scans with contrast remains to be evaluated.

As our findings suggest, the current study has a number of strengths. Inspiratory CT scans are common in clinical settings, and our method allows for the detection of functional small airway disease by using them to create virtual expiratory scans. Large-scale characterization and phenotyping of individuals with small airways disease has been limited due to the fact that fSAD^{PRM} requires RV scans which are not routinely acquired in most settings. Also, retrospective evaluation of individuals with a TLC scan but no expiratory scan is not possible. The proposed method addresses these concerns by allowing an assessment of fSAD in patient cohorts with only

TLC scans, an example being the National Lung Screening Trial (NLST) (19). Our method can also be used for the retrospective evaluation of large patient cohorts where expiratory chest CT scans were not acquired, an instance being the Multi-Ethnic Study of Atherosclerosis (MESA) (18). Also, this method has the potential to reduce radiation exposure to patients in future studies of small airway disease.

Acknowledgements

The authors thank the SPIROMICS participants and participating physicians, investigators, and staff for making this research possible. More information about the study and how to access SPIROMICS data is available at www.spiromics.org. The authors would like to acknowledge the University of North Carolina at Chapel Hill BioSpecimen Processing Facility for sample processing, storage, and sample disbursements (<http://bsp.web.unc.edu/>).

We would like to acknowledge the following current and former investigators of the SPIROMICS sites and reading centers: Neil E Alexis, MD; Wayne H Anderson, PhD; Mehrdad Arjomandi, MD; Igor Barjaktarevic, MD, PhD; R Graham Barr, MD, DrPH; Patricia Basta, PhD; Lori A Bateman, MSc; Surya P Bhatt, MD; Eugene R Bleecker, MD; Richard C Boucher, MD; Russell P Bowler, MD, PhD; Stephanie A Christenson, MD; Alejandro P Comellas, MD; Christopher B Cooper, MD, PhD; David J Couper, PhD; Gerard J Criner, MD; Ronald G Crystal, MD; Jeffrey L Curtis, MD; Claire M Doerschuk, MD; Mark T Dransfield, MD; Brad Drummond, MD; Christine M Freeman, PhD; Craig Galban, PhD; MeiLan K Han, MD, MS; Nadia N Hansel, MD, MPH; Annette T Hastie, PhD; Eric A Hoffman, PhD; Yvonne Huang, MD; Robert J Kaner, MD; Richard E Kanner, MD; Eric C Kleerup, MD; Jerry A Krishnan, MD, PhD; Lisa M LaVange, PhD; Stephen C Lazarus, MD; Fernando J Martinez, MD, MS; Deborah A Meyers, PhD; Wendy C Moore, MD; John D Newell Jr, MD; Robert Paine, III, MD; Laura Paulin, MD, MHS; Stephen P Peters, MD, PhD; Cheryl Pirozzi, MD; Nirupama Putcha, MD, MHS; Elizabeth C Oelsner, MD, MPH; Wanda K O'Neal, PhD; Victor E Ortega, MD, PhD; Sanjeev Raman, MBBS, MD; Stephen I. Rennard, MD; Donald P Tashkin, MD; J Michael Wells, MD; Robert A Wise, MD; and Prescott G Woodruff, MD, MPH. The project officers from the Lung Division of the National Heart, Lung, and Blood Institute were Lisa Postow, PhD, and Lisa Viviano, BSN; SPIROMICS was supported

by contracts from the NIH/NHLBI (HHSN268200900013C, HHSN268200900014C, HHSN268200900015C, HHSN268200900016C, HHSN268200900017C, HHSN268200900018C, HHSN26820-0900019C, HHSN268200900020C), grants from the NIH/NHLBI (U01 HL137880 and U24 HL141762), and supplemented by contributions made through the Foundation for the NIH and the COPD Foundation from AstraZeneca/MedImmune; Bayer; Bellerophon Therapeutics; Boehringer-Ingelheim Pharmaceuticals, Inc.; Chiesi Farmaceutici S.p.A.; Forest Research Institute, Inc.; GlaxoSmithKline; Grifols Therapeutics, Inc.; Ikaria, Inc.; Novartis Pharmaceuticals Corporation; Nycomed GmbH; ProterixBio; Regeneron Pharmaceuticals, Inc.; Sanofi; Sunovion; Takeda Pharmaceutical Company; and Theravance Biopharma and Mylan.

This work was supported by NHLBI grants U01 HL089897 and U01 HL089856 and by NIH contract 75N92023D00011. The COPDGene study (NCT00608764) has also been supported by the COPD Foundation through contributions made to an Industry Advisory Committee that has included AstraZeneca, Bayer Pharmaceuticals, Boehringer-Ingelheim, Genentech, GlaxoSmithKline, Novartis, Pfizer, and Sunovion.

Tables

Table 1: Participant characteristics from the SPIROMICS and COPDGene cohorts at baseline.

	SPIROMICS	COPDGene	P Value
	(n = 1458)	(n = 458)	
Age, years	62.86 (9.13)	63.30 (8.52)	0.6
Race			< 0.001
White	1,138 (78%)	454 (99%)	
Non-White	320 (22%)	4 (0.9%)	
Sex			0.008
Male	788 (54%)	215 (47%)	
Female	670 (46%)	243 (53%)	
BMI, kg / m ²	28.08 (5.18)	29.93 (6.16)	< 0.001
Smoking status			< 0.001
Former or never smokers	870 (60%)	328 (72%)	
Current smokers	588 (40%)	130 (28%)	
Smoking pack years	46.62 (28.11)	39.42 (23.77)	< 0.001
Postbronchodilator FEV ₁ , L	2.29 (0.87)	2.50 (0.75)	< 0.001
FEV ₁ / FVC ratio	0.64 (0.15)	0.71 (0.12)	< 0.001
GOLD stage			< 0.001
0	579 (40%)	240 (52%)	
1	165 (11%)	44 (9.6%)	
2	468 (32%)	78 (17%)	
3	164 (11%)	25 (5.5%)	
4	33 (2.3%)	1 (0.2%)	
Never smokers	49 (3.4%)	18 (3.9%)	
PRISm	NA	52 (11%)	
Total SGRQ score	30.18 (20.48)	12.48 (15.26)	< 0.001
6MWD, ft	1,342.01 (361.23)	1,599.13 (336.83)	< 0.001
mMRC dyspnea scale	0.95 (0.95)	0.64 (1.05)	< 0.001
fSAD ^{PRM} , %	13.35 (12.21)	10.13 (9.46)	< 0.001
fSAD ^{TLC} , %	12.98 (13.25)	9.55 (10.99)	0.002
CT emphysema (LAA < -950 HU), %	6.59 (9.07)	3.84 (5.88)	< 0.001

Data reported as mean (SD) or n (%). SPIROMICS = SubPopulations and InteRmediate Outcome Measure In COPD; COPDGene = Genetic Epidemiology of COPD; BMI = body-mass index (kg / m²); FEV₁ = forced expiratory volume in 1 second; FVC = forced vital capacity; GOLD = Global Initiative for Obstructive Lung Disease; PRISm = preserved ratio impaired spirometry; SGRQ = St. George's Respiratory Questionnaire; 6MWD = six minute walk distance (ft); mMRC = modified Medical Research Council; fSAD = functional small airways disease; TLC = total lung capacity; PRM = parametric response mapping; CT = computed tomography; LAA = low-attenuation areas (%). P values were generated using Wilcoxon's rank sum test or Pearson's Chi-squared test.

Table 2: Multivariable linear regression analysis for assessing associations of baseline fSAD^{TLC} with lung function and respiratory morbidity in SPIROMICS (Estimate, 95% CI, P Value).

	fSAD ^{TLC}	P Value	fSAD ^{PRM}	P Value
Postbronchodilator FEV ₁ , L	-0.034 (-0.037, -0.031)	<i>P</i> < 0.001	-0.034 (-0.037, -0.030)	<i>P</i> < 0.001
Postbronchodilator FEV ₁ / FVC	-0.008 (-0.008, -0.007)	<i>P</i> < 0.001	-0.007 (-0.008, -0.007)	<i>P</i> < 0.001
SGRQ	0.240 (0.127, 0.353)	<i>P</i> < 0.001	0.177 (0.064, 0.290)	0.002
6MWD, ft	-1.364 (-3.548, 0.819)	0.22	-1.887 (-4.057, 0.284)	0.09
mMRC Dyspnea Scale	0.011 (-0.002, 0.024)	0.10	0.01 (-0.003, 0.023)	0.12

CI = confidence interval; fSAD = functional small airways disease; TLC = total lung capacity; FEV₁ = forced expiratory volume in 1 second; FVC = forced vital capacity; SGRQ = St. George's Respiratory Questionnaire; 6MWD = six-minute walk distance; mMRC = modified Medical Research Council. Multivariable models were adjusted for age, sex, race, smoking status, smoking pack years, body-mass index (BMI), baseline postbronchodilator FEV₁, and percent emphysema define as percent LAA < -950 Hounsfield units (HU).

Table 3: Multivariable associations of baseline fSAD^{TLC} with lung function, symptom burden, and exercise capacity in the COPDGene cohort (Estimate, 95% CI, P Value).

	fSAD ^{TLC}	P Value	fSAD ^{PRM}	P Value
Postbronchodilator FEV ₁ , L	-0.032 (-0.038, -0.027)	<i>P</i> < 0.001	-0.032 (-0.038, -0.026)	<i>P</i> < 0.001
Postbronchodilator FEV ₁ / FVC	-0.007 (-0.008, -0.007)	<i>P</i> < 0.001	-0.007 (-0.008, -0.006)	<i>P</i> < 0.001
SGRQ	0.190 (0.030, 0.350)	0.02	0.131 (-0.043, 0.304)	0.14
6MWD, ft	-2.211 (-5.755, 1.332)	0.22	-2.505 (-6.332, 1.321)	0.20
mMRC Dyspnea Scale	0.004 (-0.023, 0.03)	0.76	-0.008 (-0.037, 0.021)	0.60

CI = confidence interval; fSAD = functional small airways disease; TLC = total lung capacity; FEV₁ = forced expiratory volume in 1 second; FVC = forced vital capacity; SGRQ = St. George's Respiratory Questionnaire; 6MWD = six-minute walk distance; mMRC = modified Medical Research Council. Multivariable models were adjusted for age, sex, race, smoking status, smoking pack years, body-mass index (BMI), baseline postbronchodilator FEV₁, and percent emphysema define as percent LAA < -950 Hounsfield units (HU).

Table 4: Association between fSAD^{TLC} and change in FEV₁ (mL / year) stratified by baseline COPD GOLD stage (Estimate, 95% CI, *P* Value).

		fSAD ^{TLC}	<i>P</i> Value	fSAD ^{PRM}	<i>P</i> Value
SPIROMICS	Overall	-1.156 (-1.699, -0.613)	<i>P</i> < 0.001	-0.742 (-1.280, -0.205)	0.007
	GOLD 0	-2.994 (-5.900, -0.088)	0.04	-0.084 (-1.244, 1.077)	0.89
	GOLD 1 - 4	-1.050 (-1.691, -0.408)	0.001	-0.899 (-1.598, -0.201)	0.01
COPDGene	Overall	-0.866 (-1.386, -0.345)	0.001	-0.871 (-1.440, -0.303)	0.003
	GOLD 0	-0.230 (-1.760, 1.300)	0.77	-0.514 (-1.845, 0.817)	0.45
	GOLD 1 - 4	-1.175 (-1.943, -0.406)	0.003	-1.067 (-1.934, -0.200)	0.02

CI = confidence interval; fSAD = functional small airways disease; TLC = total lung capacity; GOLD = Global Initiative for Obstructive Lung Disease; FEV₁ = forced expiratory volume in 1 second. Multivariable models were adjusted for age, sex, race, smoking status, smoking pack years, body-mass index (BMI), baseline postbronchodilator FEV₁, and percent emphysema define as percent LAA < -950 Hounsfield units (HU).

Figures

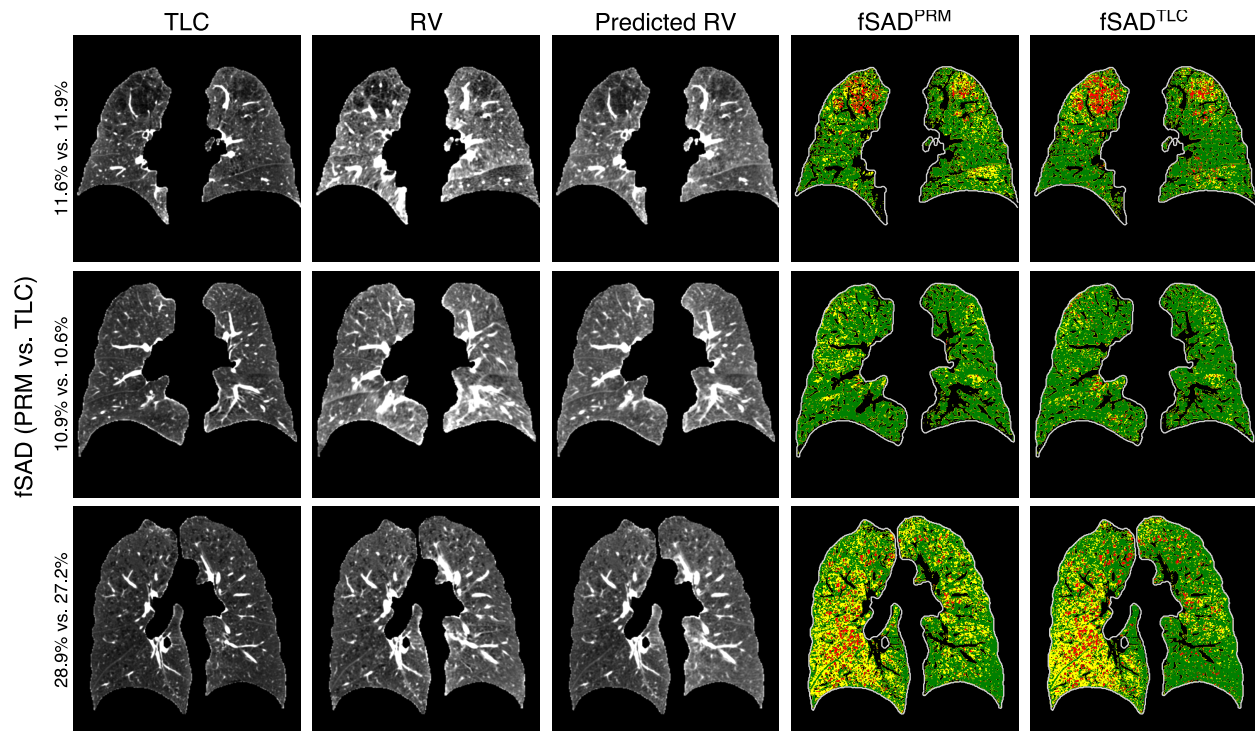


Figure 1: Spatial distribution of fSAD^{PRM} and fSAD^{TLC}, shown on mid-coronal slices from three different individuals with varying degrees of small airways disease. The first and the second columns indicate chest CT scans at total lung capacity (TLC) and residual volume (RV), respectively. The TLC and RV scans were used to compute fSAD^{PRM}. The third column shows the virtual or synthetic RV scans generated from the TLC chest CT scan alone. fSAD^{TLC} was computed using the TLC scan and the virtual RV scan, which allowed for a single-volume estimation of fSAD from TLC alone.

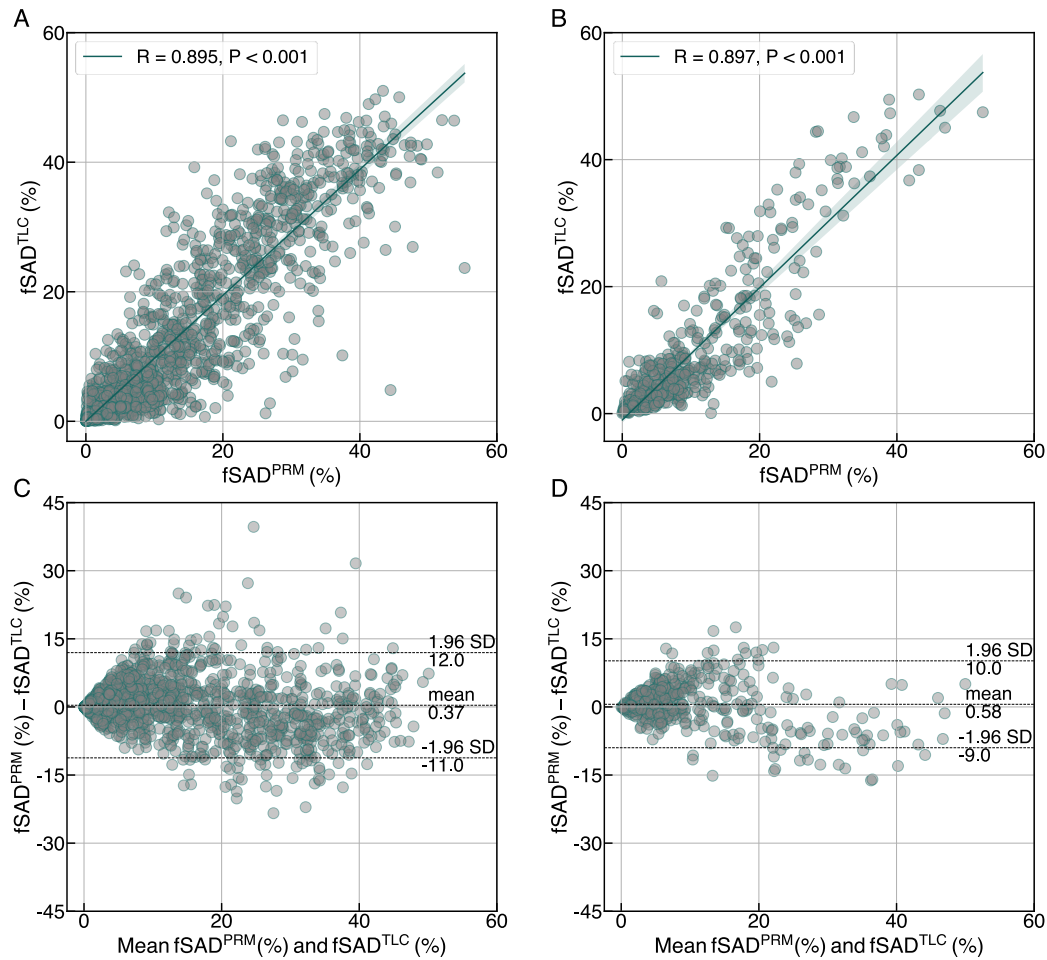


Figure 2: Relationship between fSAD^{TLC} with fSAD^{PRM} in both (A and C) SPIROMICS ($n = 1458$) and (B and D) COPDGene ($n = 458$) cohorts through scatter plots and Bland-Altman analysis. Pearson's correlation, R is also reported for both cohorts.

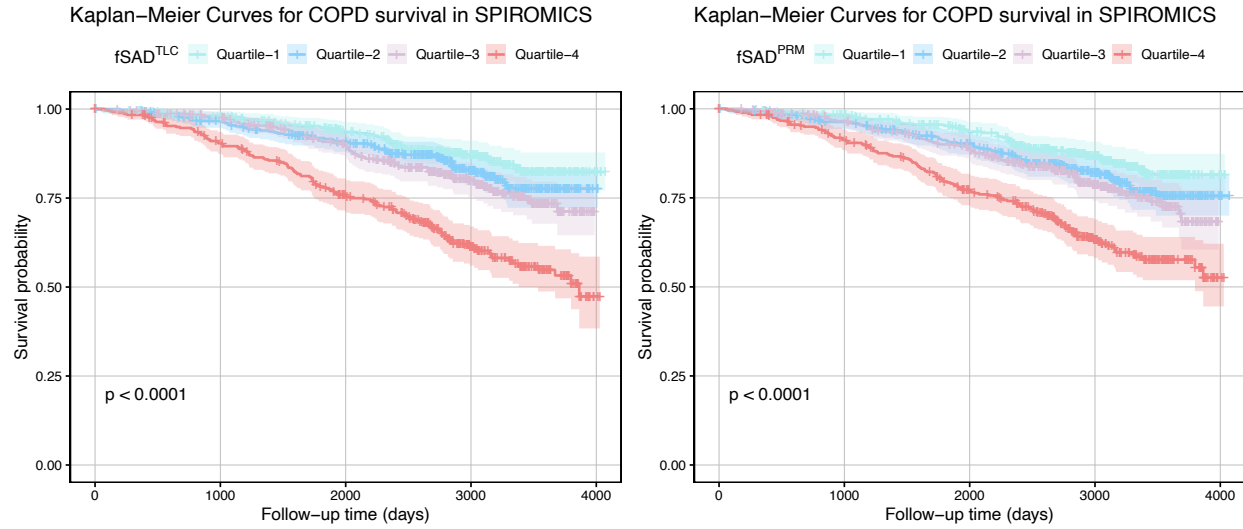


Figure 3: Kaplan-Meier curve analysis for studying overall survival in different quartiles of fSAD^{TLC} in both (A) SPIROMICS and (B) COPDGene cohorts.

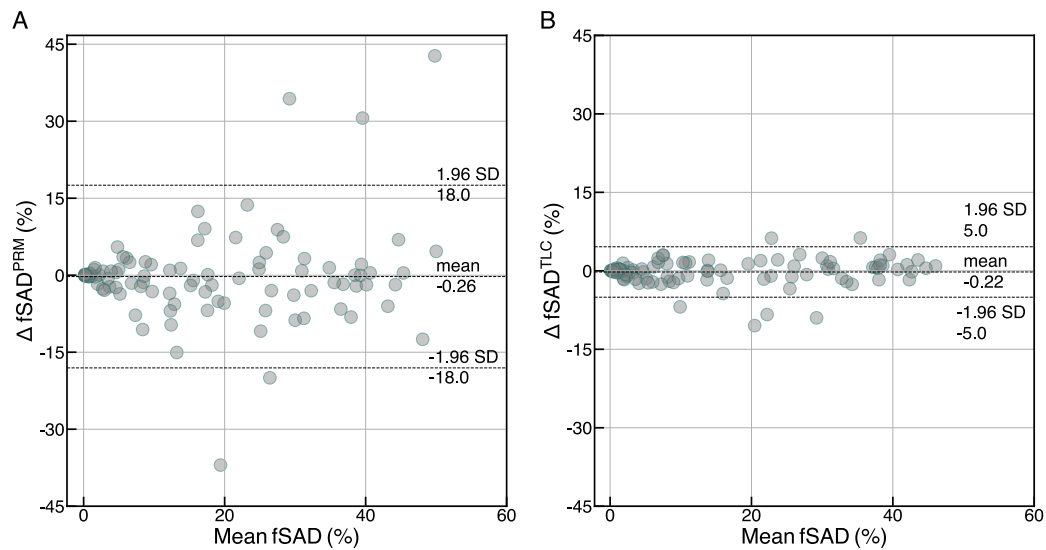


Figure 4: Repeatability study of (A) fSAD^{PRM} and (B) fSAD^{TLC} between baseline and 2 to- 6-week follow-up ($n = 98$) through Bland-Altman analysis.

References

1. Hogg JC, Macklem PT, Thurlbeck WM. Site and Nature of Airway Obstruction in Chronic Obstructive Lung Disease. *N Engl J Med* 1968;278:1355–1360.
2. Yanai M, Sekizawa K, Ohru T, Sasaki H, Takishima T. Site of airway obstruction in pulmonary disease: direct measurement of intrabronchial pressure. *J Appl Physiol* 1992;72:1016–1023.
3. Koo H-K, Vasilescu DM, Booth S, Hsieh A, Katsamenis OL, Fishbane N, *et al.* Small airways disease in mild and moderate chronic obstructive pulmonary disease: a cross-sectional study. *Lancet Respir Med* 2018;6:591–602.
4. Galbán CJ, Han MK, Boes JL, Chughtai KA, Meyer CR, Johnson TD, *et al.* Computed tomography–based biomarker provides unique signature for diagnosis of COPD phenotypes and disease progression. *Nat Med* 2012;18:1711–1715.
5. Vasilescu DM, Martinez FJ, Marchetti N, Galbán CJ, Hatt C, Meldrum CA, *et al.* Noninvasive Imaging Biomarker Identifies Small Airway Damage in Severe Chronic Obstructive Pulmonary Disease. *Am J Respir Crit Care Med* 2019;200:575–581.
6. Comellas AP, Newell JD, Kirby M, Sieren JP, Peterson S, Hatt C, *et al.* Residual Volume versus FRC Computed Tomography Assessment of Functional Small Airway Disease in Smokers with and without Chronic Obstructive Pulmonary Disease. *Am J Respir Crit Care Med* 2023;207:1536–1539.
7. Chaudhary MFA, Gerard SE, Christensen GE, Cooper CB, Schroeder JD, Hoffman EA, *et al.* LungViT: Ensembling Cascade of Texture Sensitive Hierarchical Vision Transformers for Cross-Volume Chest CT Image-to-Image Translation. *IEEE Trans Med Imaging* 2024;43:2448–2465.

8. Couper D, LaVange LM, Han ML, Barr RG, Bleecker E, Hoffman EA, *et al.* Design of the subpopulations and intermediate outcomes in copd study (SPIROMICS). *Thorax* 2014;doi:10.1136/thoraxjnl-2013-203897.
9. Regan EA, Hokanson JE, Murphy JR, Make B, Lynch DA, Beaty TH, *et al.* Genetic epidemiology of COPD (COPDGene) study design. *COPD J Chronic Obstr Pulm Dis* 2010;doi:10.3109/15412550903499522.
10. Pompe E, Galbán CJ, Ross BD, Koenderman L, Ten Hacken NH, Postma DS, *et al.* Parametric response mapping on chest computed tomography associates with clinical and functional parameters in chronic obstructive pulmonary disease. *Respir Med* 2017;123:48–55.
11. Jones PW. St. George’s Respiratory Questionnaire: MCID. *COPD J Chronic Obstr Pulm Dis* 2005;2:75–79.
12. Mahler DA, Wells CK. Evaluation of Clinical Methods for Rating Dyspnea. *Chest* 1988;93:580–586.
13. Ranstam J, Cook JA, editors. Kaplan–Meier curve. *Br J Surg* 2017;104:442–442.
14. Motahari A, Barr RG, Han MK, Anderson WH, Barjaktarevic I, Bleecker ER, *et al.* Repeatability of Pulmonary Quantitative Computed Tomography Measurements in Chronic Obstructive Pulmonary Disease. *Am J Respir Crit Care Med* 2023;208:657–665.
15. Weir JP. Quantifying Test-Retest Reliability Using the Intraclass Correlation Coefficient and the SEM. *J Strength Cond Res* 2005;19:231.
16. Bhatt SP, Soler X, Wang X, Murray S, Anzueto AR, Beaty TH, *et al.* Association between Functional Small Airway Disease and FEV₁ Decline in Chronic Obstructive Pulmonary Disease. *Am J Respir Crit Care Med* 2016;194:178–184.

17. Brown MS, Kim HJ, Abtin F, Da Costa I, Pais R, Ahmad S, *et al.* Reproducibility of Lung and Lobar Volume Measurements Using Computed Tomography. *Acad Radiol* 2010;17:316–322.
18. Bild DE. Multi-Ethnic Study of Atherosclerosis: Objectives and Design. *Am J Epidemiol* 2002;156:871–881.
19. National Lung Screening Trial Research Team. The National Lung Screening Trial: Overview and Study Design. *Radiology* 2011;258:243–253.